

INVESTIGATION OF THE RIES IMPACT CRATER BASED UPON OLD AND NEW GEOPHYSICAL DATA AND NUMERICAL MODELING. K. Wünnemann¹ and J. V. Morgan¹, ¹Department of Earth Science and Engineering, Imperial College London, London SW7 2AZ, UK, k.wunnemann@imperial.ac.uk, j.morgan@imperial.ac.uk.

Introduction: The lack of consistency between similar-sized craters on Earth makes it difficult to define typical structural elements for a given size range. The fact that most terrestrial craters are not pristine might be one reason for the lack of similarities. Post-impact modifications like erosion and tectonic overprinting can prevent, in many cases, an accurate reconstruction of the original crater morphology. Another reason might be varying material properties at different impact sites. The composition of the upper crust on Earth is presumably more complex than on any other planetary body. We assume that this has an essential effect on the formation process and we suppose that it is at least partially responsible for the lack of structural similarity between similar-sized craters.

In order to evaluate the size of terrestrial craters and to understand the formational process it is crucial to know whether a particular crater is a relatively typical example for its size range or whether the formation of the structure was heavily influenced by local target conditions. Considering the Ries crater as an example for middle-sized complex impact structures on Earth we use geophysical data to examine the structure underneath the crater. In order to investigate the influence of varying target compositions on the cratering process and the final crater morphology we utilize numerical modeling technique to simulate the formation process and to evaluate whether Ries was formed under 'normal' conditions.

The Ries Crater: The Ries crater is a middle-sized complex crater in Germany 15 Ma old. Due to relatively low erosion rates in this area it is well preserved. The crater was intensively investigated [1] making Ries to one of the best-studied craters on Earth. The crater is characterized by an almost circular relatively flat inner basin, 12 km in diameter surrounded by a so called crystalline inner ring and an outer tectonic ridge representing a system of concentric normal faults with a maximum extension of approximately 24 km in diameter.

Seismic refraction analysis. Several seismic refraction profiles have been acquired across the crater [2,3]. In most analyses of these data the authors concluded that average velocities inside the crater are lower than those outside, and that this low-velocity zone extends to 3-6 km below the subsurface [1,3]. The objective of re-analyzing the refraction data was to investigate the apparent absence of structural uplift beneath the crater.

We agree with previous investigations that the average velocity inside the crater is lower than outside the crater from the surface to ~2.2 km depth, but that below this level velocity increases beneath the center presumably due to uplifted basement rocks by ~1 km (Fig. 1).

Magnetotelluric investigation. In order to investigate the deep structure beneath Ries crater we utilized MT depth sounding. 2D inversion models of the data show anomalously high conductivity beneath the crater. Our most supported model (Fig. 4) featuring a highly conductive zone to a depth of ~2 km is consistent with the interpretation of the seismic refraction as well as of gravimetric data [4]. The high conductivity can be explained by brine-filled fractures in open pore space.

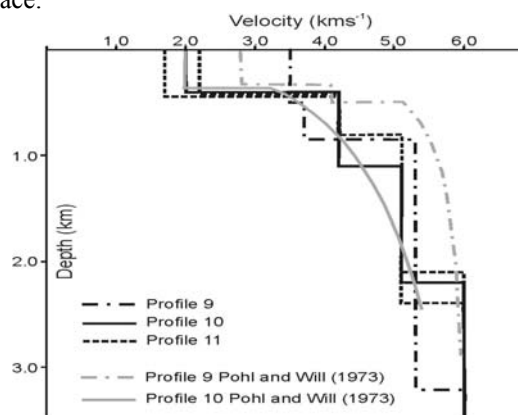


Fig. 1. P-wave velocity-depth profiles determined from modeling of first arrival-times for Profile 9 (outside the crater) and 10 and 11 (inside the crater). For comparison, velocity models for Profiles 9 and 10 from [3] are also displayed.

Numerical Modeling: In addition we present a numerical model (SALE Hydrocode [5,6]) of the formation of Ries crater which is consistent with surface (crater morphology) and subsurface (fragmentation zone, central uplift) observations in the vicinity of the crater (Fig 2 A). In order to explain the structural differences between similar-sized craters and Ries we investigate the influence of varying target compositions (sedimentary layer and crystalline basement feature different thermodynamic and mechanical properties) on the cratering process and the final crater morphology. For a reasonable range of constitutive material properties the model calculations produce a large variety of different crater shapes, even for the same amount of impact energy (Fig. 2). Utilizing acoustic

fluidization [6,7] as the major weakening mechanism of target rocks during crater formation shows that the range of sensible model parameters (block size, vibration time) results in different crater morphologies showing different stages of strutral uplift (Fig. 3).

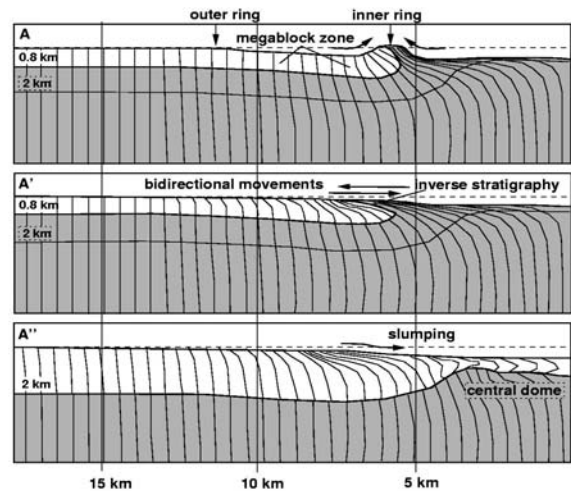


Fig. 2. Comparison of the final crater shape of three models utilizing different strength properties (cohesion C_s , friction coefficient ϕ_s) and spatial extensions (l) of the upper (sedimentary) layer. Model A (best-fit): $l=0.8$ km, $C_s=10$ MPa, $\phi_s=0.9$; Model A': $l=0.8$ km, $C_s=0$ MPa, $\phi_s=0.5$; Model A'': $l=2$ km, $C_s=0$ MPa, $\phi_s=0.5$.

Conclusion: The numerical models testify that the final crater shape is very sensitive to the properties of the target rocks. Sedimentary material is assumed to be weaker (less resistant against shear failure) than crystalline basement rocks. For this reason craters formed in sedimentary target compositions are relatively flat, whereas craters in mainly crystalline rocks exhibit more pronounced structural elements. In this regard Ries crater morphology is more similar to the latter case, whereas the presence of a sedimentary layer might have supported the formation of the well pronounced megablock zone. Apart from matching the surface structure, our model is also consistent with the geophysical observations of the subsurface and it appears to be most likely that both processes fragmentation and structural uplift of dense basement material accompanied the formation of Ries crater.

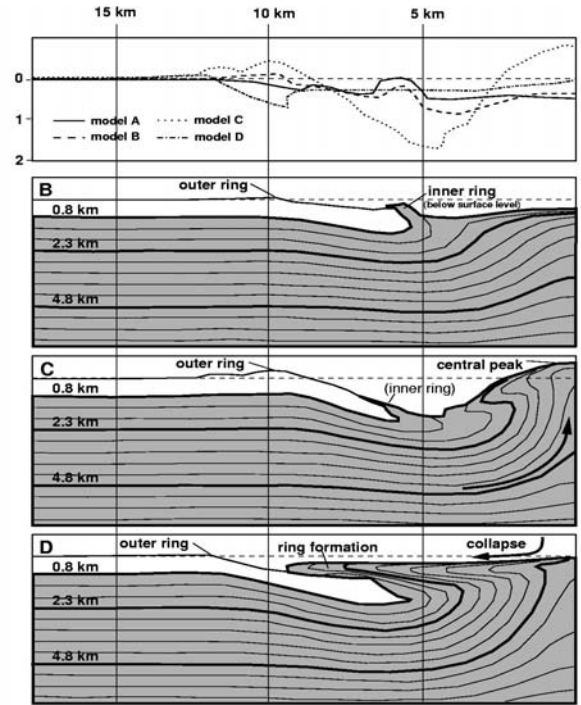


Fig. 3. Comparison of the final crater shape (B; C, D) utilizing different acoustic fluidization parameters. The upper diagram shows a comparison of the final crater topography of models A,B,C,D (see Fig. 2).

Acknowledgements: We are gratefully thankful to J. Pohl, providing the seismic refraction data, H. Jödicke and A. Jording for their help with the MT-measurements. This work was supported by the DFG.

References: [1] Pohl J. et al. (1977) in *Impact and Explosion Cratering*, 343–404. [2] Angenheister G. and Pohl J. (1969) *Geologica Bavarica*, 61, 304-326. [3] Pohl J. and Will M. (1974) *Geologica Bavarica*, 72, 75–80. [4] Kahle H.-G. (1969) *Geologica Bavarica*, 35, 317-345. [5] Amsden A. A. Et al. (1980) *LA-8095 Report*, Los Alamos National Lab., 101 p.. [6] Wünnemann K. and Ivanov B. A. (2003) *Plan. Space Science*, 51, 831-845. [5] Melosh H. J. (1979) *JGR*, 84, 7513-7520.

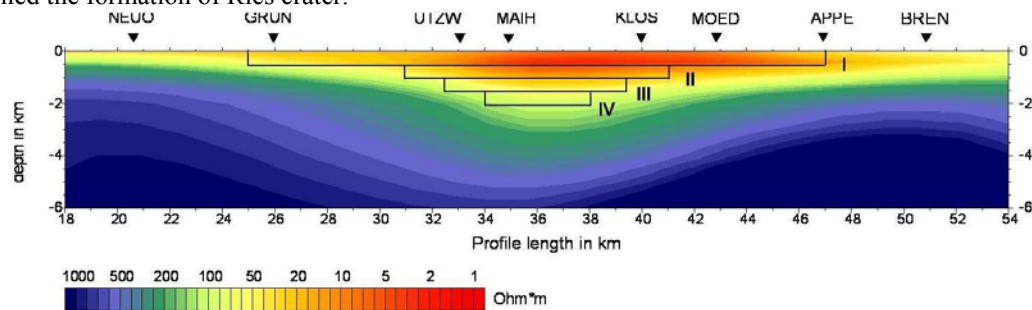


Fig. 4. Comparison between MT model and gravity model consisting of cylindric layers, redrawn after [4].